Mathematical Biosciences and Engineering

MBE, 20(2): 4153–4177.
DOI: 10.3934/mbe.2023194
Received: 27 September 2022
Revised: 11 November 2022
Accepted: 16 November 2022
Published: 21 December 2022

http://www.aimspress.com/journal/MBE

Research article

Identifying key transcription factors and miRNAs coregulatory networks associated with immune infiltrations and drug interactions in idiopathic pulmonary arterial hypertension

Qian Li[1], Minawaer Hujiaaihemaiti[1], Jie Wang[2], Md. Nazim Uddin[3], Ming-Yuan Li[1], Alidan Aierken[1] and Yun Wu[1,*]

[1] Department of General Medicine, First Affiliated Hospital of Xinjiang Medical University, Urumqi 830011, China
[2] Department of Pharmacy, First Affiliated Hospital of Xinjiang Medical University, Urumqi 830011, China
[3] Institute of Food Science and Technology, Bangladesh Council of Scientific and Industrial Research (BCSIR), Dhaka 1205, Bangladesh

*** Corresponding author:** Email: wuyun8009@163.com.

Abstract: Background: The deregulated genetic factors are critically associated with idiopathic pulmonary arterial hypertension (IPAH) development and progression. However, the identification of hub-transcription factors (TFs) and miRNA-hub-TFs co-regulatory network-mediated pathogenesis in IPAH remains lacking. Methods: We used GSE48149, GSE113439, GSE117261, GSE33463, and GSE67597 for identifying key genes and miRNAs in IPAH. We used a series of bioinformatics approaches, including R packages, protein-protein interaction (PPI) network, and gene set enrichment analysis (GSEA) to identify the hub-TFs and miRNA-hub-TFs co-regulatory networks in IPAH. Also, we employed a molecular docking approach to evaluate the potential protein-drug interactions. Results: We found that 14 TFs encoding genes, including ZNF83, STAT1, NFE2L3, and SMARCA2 are upregulated, and 47 TFs encoding genes, including NCOR2, FOXA2, NFE2, and IRF5 are downregulated in IPAH relative to the control. Then, we identified the differentially expressed 22 hub-TFs encoding genes, including four upregulated (STAT1, OPTN, STAT4, and SMARCA2) and 18 downregulated (such as NCOR2, IRF5, IRF2, MAFB, MAFG, and MAF) TFs encoding genes in IPAH. The deregulated hub-TFs regulate the immune system, cellular transcriptional signaling, and cell cycle regulatory pathways. Moreover, the identified differentially

expressed miRNAs (DEmiRs) are involved in the co-regulatory network with hub-TFs. The six hub-TFs encoding genes, including STAT1, MAF, CEBPB, MAFB, NCOR2, and MAFG are consistently differentially expressed in the peripheral blood mononuclear cells of IPAH patients, and these hub-TFs showed significant diagnostic efficacy in distinguishing IPAH cases from the healthy individuals. Moreover, we revealed that the co-regulatory hub-TFs encoding genes are correlated with the infiltrations of various immune signatures, including CD4 regulatory T cells, immature B cells, macrophages, MDSCs, monocytes, Tfh cells, and Th1 cells. Finally, we discovered that the protein product of STAT1 and NCOR2 interacts with several drugs with appropriate binding affinity. Conclusions: The identification of hub-TFs and miRNA-hub-TFs co-regulatory networks may provide a new avenue into the mechanism of IPAH development and pathogenesis.

Keywords: IPAH; Co-regulatory network; TFs; immune signatures; binding affinity

1. Introduction

Pulmonary hypertension (PAH) is a crucial health issue for older people worldwide [1]. PAH is commonly associated with various diseases and infectious diseases, including congenital heart disease, rheumatic heart disease, HIV and schistosomiasis [1]. PAH is frequently correlated with patients' clinical deterioration and mortality risk [2]. In PAH, the increased pulmonary arterial pressure is associated with right ventricle failure, which in turn is associated with the premature death of patients [3]. Several types of PAH include IPAH, familial pulmonary arterial hypertension, PAH with significant venous or capillary involvement, and PAH associated with other diseases [4]. There are various causes for developing progressive PAH. However, no known causes are labeled for the pathogenesis of idiopathic IPAH [2,3]. IPAH is characterized histopathologically by angioproliferative plexiform lesions of endothelial cells, muscularization of precapillary arterioles, intimal endothelial cell proliferation and medial thickening due to vascular smooth muscle cell proliferation [4]. In IPAH, the pulmonary artery pressure is persistently more than 25 mmHg at rest and more than 30 mmHg during exercise [5]. IPAH is associated with various clinical complications, including pulmonary vascular resistance, right ventricular dysfunction, exercise limitation, failure of the right heart and premature death [6,7]. In addition, nocturnal hypoxia is associated with the pathogenesis of IPAH [8]. There are numerous non-specific symptoms, including breathing shortness, angina, weakness and syncope for IPAH patients [2,3].

Some of the previous studies provide the clue that genetic factors [9], including gene defects, gene rearrangements and mutation are associated with the development and progression of IPAH. For example, BMPR2 gene rearrangements are crucially associated with the pathogenesis of IPAH [10]. In IPAH, loss-of-function mutation of the BMPR2 gene and exaggerated activation of TGF-β signaling is associated with increased bone morphogenetic deregulated protein signaling [11]. It was stated that the BMPR1B (ALK6) mutations are associated with the pathogenesis of childhood IPAH [12]. The same authors discovered that the mutations of endoglin, SMAD1, SMAD2, SMAD3, SMAD4, SMAD5, SMAD6, SMAD7 and BMPR1A genes in 43 IPAH patients [12]. Moreover, numerous TFs are deregulated in idiopathic pulmonary arterial hypertension [13]. For example, the SOX17 gene is critically correlated to the pulmonary vasculature and the pathobiology of PAH [14]. Park et al. [15] demonstrated that downregulated levels of Sox17 in pulmonary arterioles augmented the

susceptibility to PAH via upregulation of HGF/c-Met signaling. Wang et al. [16] revealed that SOX17 loss-of-function mutation is related to the molecular pathogenesis of PAH. The novel risk gene SOX17 contributed to PAH-congenital heart disease and idiopathic/familial PAH [17]. Yuan et al. [18] found that an elevated level of RUNX2 is an independent predictor for the survival of IPAH patients and is associated with the clinical severity of IPAH. However, the molecular mechanisms of IPAH are poorly understood, and the deregulated immunological activities are crucial factors in IPAH pathogenesis and development. The differentiated levels of immune cells, such as T lymphocytes, dendritic cells, B cells, macrophages, monocytes, neutrophils and mast cells are found in the IPAH [2,19]. Zeng et al. [20] identified the biomarkers involved with the immune infiltration characteristics in IPAH. In addition to the genetic coding factors, non-coding genetic materials, including miRNAs are involved with the development, pathogenesis and progression of IPAH [21]. He et al. [22] demonstrated that mRNAs are potential circulating biomarkers and contribute to the pathophysiology of IPAH. Sarrion et al. [21] found that the expression level of miR-23a is associated with the patient's pulmonary function. Li et al. [23] identified the miRNA-mRNA network potentially related to the pathogenesis of IPAH. Hao et al [24] identified the IPAH-related miRNA-mRNA regulatory network associated with the pathogenesis. These previous studies provide potential suggestions regarding the association of coding and non-coding genetic factors with developing the pathogenesis of IPAH. Therefore, global efforts are mandatory to reveal the crucial genes and miRNAs that are critically associated with IPAH pathogenesis and development. Moreover, the potential drug-gene interaction should be elucidated for treating IPAH.

2. Materials and methods

2.1. Collection of datasets

We followed the methods structure of Li et al. [25] 2021 and searched the NCBI gene expression omnibus (GEO) database (https://www.ncbi.nlm.nih.gov/geo/) by using the keywords "PAH", "IPAH", "pulmonary arterial hypertension", "arterial hypertension", "pulmonary hypertension", "idiopathic pulmonary arterial hypertension", "blood in pulmonary arterial hypertension" and "roles of blood in pulmonary arterial hypertension", and identified the three mRNA expression datasets associated with idiopathic pulmonary arterial hypertension from a different platform. The mRNA expression datasets were GSE48149 (https://www.ncbi.nlm.nih.gov/geo/query/acc.cgi?acc=GSE48149) [26,27], GSE113439 (https://www.ncbi.nlm.nih.gov/geo/query/acc.cgi?acc=GSE113439) [28], and GSE117261 (https://www.ncbi.nlm.nih.gov/geo/query/acc.cgi?acc=GSE117261) [29,30]. Moreover, we downloaded the gene expression data GSE33463 (https://www.ncbi.nlm.nih.gov/geo/query/acc.cgi?acc=GSE33463) [31] for validating the results. Furthermore, we downloaded the miRNA expression data GSE67597 (https://www.ncbi.nlm.nih.gov/geo/query/acc.cgi?acc=GSE67597) [32] for identifying the differentially expressed miRNA in idiopathic pulmonary arterial hypertension. We included the IPAH samples with respective control samples in our study and excluded other samples from the same gene expression dataset.

2.2. Identification of differentially expressed genes (DEGs) and TFs in IPAH

We integrated the three-mRNA expression datasets (GSE48149 [26,27], GSE113439 [28] and GSE117261 [29,30]) for identifying the DEGs in IPAH. We employed the NetworkAnalyst [33] software, an online-based tool (https://www.networkanalyst.ca/), to perform a meta-analysis of three IPAH-associated gene expression datasets. The selected datasets were normalized by base-2 log transformation, and we removed batch effects from multiple datasets using the ComBat method [34]. Finally, integrating the three datasets found a total of 16,874 common genes. We employed the limma R package from the Bioconductor project (http://www.bioconductor.org/) to identify DEGs [35]. The thresholds of adjusted P-value < 0.05 and $|Log2FC| > 0.65$ were set to determine the significance level. We downloaded the TFs from GSEA (https://www.gsea-msigdb.org/gsea/msigdb/human/gene_families.jsp) [36]. The online tool "Calculate and draw custom Venn diagrams" (http://bioinformatics.psb.ugent.be/webtools/Venn/) was used to identify common TF encoding genes in IPAH. Moreover, we used GSE33463 [31] to validate our findings. GSE33463 included the transcript profiles of peripheral blood mononuclear cells from 30 IPAH patients and 41 healthy individuals. We used the limma R package (http://www.bioconductor.org/) for validating the DEGs between the IPAH and healthy individuals [35].

2.3. Construction of the PPI network and Identification of the hub-TFs

The STRING (version v11 [37]), an online-based tool, was used to construct PPI networks of the significant DEGs. The hub genes were revealed using the Cytoscape plugin cytoHubba [38]. We identified hub genes with a threshold of medium interaction score ≥ 0.40 and a degree of interaction ≥ 10 in the PPI [39]. We identified hub-TFs by comparing the hub nodes with TFs using the "Calculate and draw custom Venn diagrams" (http://bioinformatics.psb.ugent.be/webtools/Venn/) tool. We used the Cytoscape (version 3.6.1) [40] tool for visualizing the PPI network.

2.4. Pathway and gene ontology (GO) analysis of hub-TFs

We performed pathway enrichment analysis of the hub-TFs that were differentially expressed in IPAH by using the GSEA software [36]. The GOs and Reactome pathways (https://reactome.org/) are identified that are significantly associated with the hub-TFs. We selected the significant GOs and Reactome pathways using a threshold of FDR < 0.05.

2.5. Identification of DEmiRs in IPAH and target genes of DemiRs

To identify the DEmiRs, we used the GEO2R tool (http://www.ncbi.nlm.nih.gov/geo/geo2r). We used the miRNA expression data GSE67597 [7] for determining the differentially expressed miRNA in idiopathic pulmonary arterial hypertension. The GEO2R tool is based on the "GEOquery" and "limma" R packages (http://www.bioconductor.org/). We selected the miRNAs with a P-value < 0.05 and $|LogFC| > 1.0$ to find out the significant level. Then, we employed another tool, the miRNet [41] for identifying the target genes of DemiRs. The "Calculate and draw custom Venn diagrams" (http://bioinformatics.psb.ugent.be/webtools/Venn/) tool was utilized to screen common genes between the target genes of DemiRs and the hub-TFs in IPAH. We used the Cytoscape (version 3.6.1) [40]

tool for visualizing the mRNA-miRNA co-regulatory network.

2.6. Exploration of Diagnostic efficacy of hub-TFs

We employed the "pROC" package of the R program for identifying the diagnostic value of hub-TFs in IPAH [42]. We used the expression value of hub-TFs in the GSE117261 [29,30] and GSE33463 [31] to compare the IPAH cases from healthy individuals. To assess the diagnostic efficacy of hub-TFs, we calculated and visualized the receiver operating characteristic (ROC) analysis and the area under the ROC curve (AUC) to identify the diagnostic efficacy of hub-TFs to differentiate IPAH cases from the normal samples. The more considerable AUC value of single hub-TFs indicates the capability of those TFs to separate the cases between IPAH and normal samples. Our study considered an AUC value greater than 0.5 with a P-value < 0.05 for taking the diagnostic hub-TFs [43].

2.7. *Exploration of the immune signature enrichment levels with hub-TFs*

We calculated the enrichment level of immune signatures in an IPAH sample as the single-sample gene-set enrichment analysis (ssGSEA) score in the GSE117261 [29,30]. We included 25 immune signatures to identify the ssGSEA score. The immune signatures included activated dendritic cells, B cells, CAFs, CD4+ regulatory T cells, CD8+ regulatory T cells, endothelial cells, eosinophil, epithelial cells, immature B cells, immature dendritic cells, M2 macrophages, macrophages, mast cells, monocytes, MDSCs, neutrophils, NK cells, pDCs, pericyte, smooth muscle cells, Tfh, Th1, Th2, Th17 and Tregs. The marker genes set of immune signatures are presented in Supplementary Table S1. We identified the differences in immune signatures between the IPAH and control samples by applying the Wilcoxon Rank-Sum Test ($P < 0.05$). Then, we identified Spearman's correlation between the expression levels of s hub-TFs and the ssGSEA score of immune signatures (the absolute value of R is not less than 0.30, $P < 0.05$). We employed Spearman's correlation test because the expression level of genes and ssGSEA score of immune signatures were not normally distributed [44].

2.8. *Identification of potential drug-hub-TFs interaction and the molecular docking of hub-TFs*

We used the DGIdb to identify the drugs targeting the hub-TFs [45]. DGIdb is based on the interaction of drug-gene data from 30 disparate sources, including Drug Bank, ChEMBL, Ensembl, NCBI Entrez, PharmGKB, PubChem, clinical trial databases, and literature in NCBI PubMed. We visualize the collected drug-gene interaction using Cytoscape software [40]. After identifying the potential drugs, we applied molecular docking analysis to identify the potential binding affinity of drugs with hub-TFs. We found the protein product of 2 hub-TFs (STAT1 (1YVL [46]) and NCOR2 (2LTP (https://www.rcsb.org/structure/2ltp)) that are potentially interacting with several drugs. We prepared proteins by using the Discovery studio (https://3ds.com/products-services/biovia/products) software. First, we discarded the water molecules and ligands from the complex proteins. Then, a molecular docking study was employed using the PyRx 0.8 (https://pyrx.sourceforge.io/), a virtual screening tool for identifying the binding affinity of drugs.

3. Results

3.1. Identification of DEGs and TFs in IPAH

We identified 927 DEGs in IPAH, including 150 upregulated genes (Supplementary Table S2) and 777 downregulated genes (Supplementary Table S3) in 3 integrated IPAH datasets relative to the control samples. Then, we overlap the TFs that are differentially expressed in IPAH. We found that 14 TFs encoding genes (ZNF83, ZNF331, TCF4, STAT1, NFE2L3, BNC2, BACH2, ZNF248, STAT4, ZNF234, OPTN, HIVEP2, NFIB and SMARCA2) are upregulated and 47 TFs encoding genes (MEFV, NCOR2, FOXA2, TTLL4, STAT5A, CBX6, TFE3, E2F4, POU2F2, SRCAP, TRMT1, HHEX, SPI1, TBX3, TRIM28, IRF2, MAFB, MAFG, MAF, MANSC1, SREBF1, MYBBP1A, TRIM62, CBFA2T3, NFE2, KLF11, RNF41, KCNIP3, ARID3A, E2F1, PACS2, ZBTB7A, CBX8, STAT6, NFIC, KEAP1, ZBTB39, HOXD1, RFXANK, TAF6L, MLX, GSX1, IRF5, MFSD12, ASCL1, UHRF1 and CEBPB) are downregulated in IPAH (Figure 1). The top ten upregulated and top ten downregulated TFs are illustrated in Table 1.

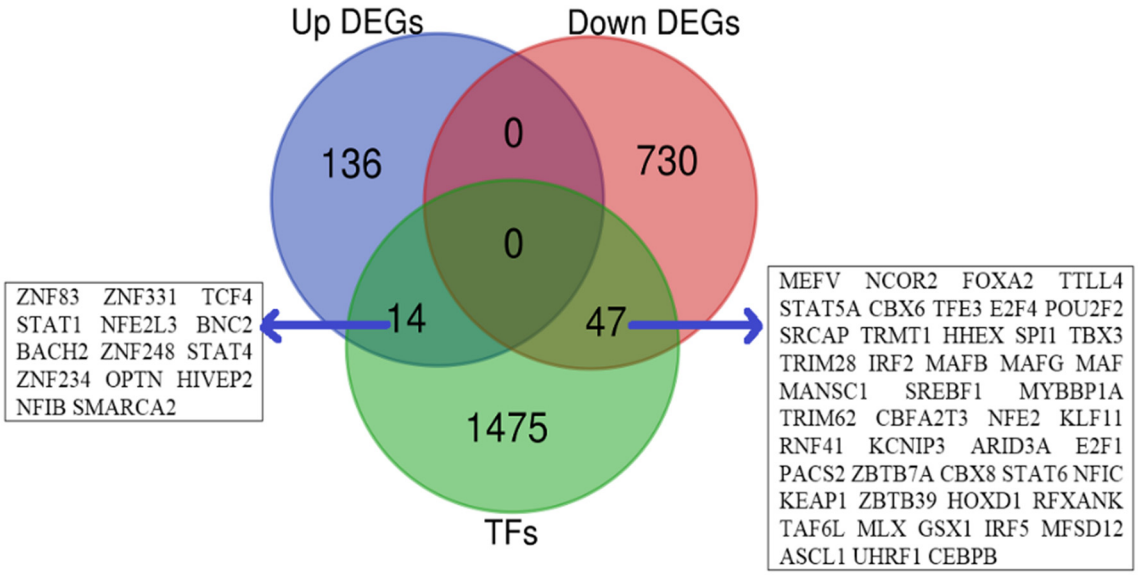

Figure 1. Upregulated 14 TFs encoding genes and downregulated 47 TFs encoding genes in IPAH. TFs indicate TFs; Up DEGs indicate upregulated DEGs; Down DEGs indicate downregulated DEGs.

Table 1. The top ten upregulated and top ten downregulated TFs in IPAH.

Regulatory status	Entrez ID	Symbol	Combined ES	P value
Upregulated	6775	STAT4	1.5946	1.16×10^{-7}
	3097	HIVEP2	1.2056	2.41×10^{-02}
	55,769	ZNF83	1.084	2.52×10^{-04}
	54,796	BNC2	1.077	3.81×10^{-02}
	6925	TCF4	0.98257	1.00×10^{-03}
	10,133	OPTN	0.95956	4.93×10^{-02}
	6595	SMARCA2	0.91287	2.67×10^{-03}
	57,209	ZNF248	0.8445	6.71×10^{-03}
	60,468	BACH2	0.80153	1.10×10^{-02}
	6772	STAT1	0.78905	3.60×10^{-02}
Downregulated	6688	SPI1	−1.3852	2.20×10^{-06}
	6720	SREBF1	−1.3275	6.26×10^{-06}
	10,629	TAF6L	−1.2937	4.32×10^{-02}
	9817	KEAP1	−1.283	1.23×10^{-04}
	30,818	KCNIP3	−1.2715	1.38×10^{-05}
	8625	RFXANK	−1.2174	2.88×10^{-02}
	23,466	CBX6	−1.1972	4.58×10^{-05}
	3663	IRF5	−1.1861	5.91×10^{-05}
	54,682	MANSC1	−1.1677	7.61×10^{-05}
	863	CBFA2T3	−1.1397	2.69×10^{-02}

3.2. Construction of PPI and identification of the hub-TFs centric PPI in IPAH

We inputted all DEGs into the STRING tools for identifying the interactions. Based on the PPI interaction of all DEGs in the STRING tool, we constructed and identified the hub genes in the IPAH. We found that the 841 DEGs are involved in the PPI, including 302 hub genes (Degree ≥ 10 and interaction ≥ 0.40) (Supplementary Table S4). Using the Venn diagram, we identified the hub-TFs encoding genes in IPAH (Figure 2A). Interestingly, we found the 22 deregulated hub-TFs encoding genes, including four upregulated (STAT1, OPTN, STAT4 and SMARCA2) and 18 downregulated (TRMT1, RNF41, SPI1, NCOR2, IRF5, E2F1, TRIM28, STAT5A, IRF2, MAFB, MAFG, MAF, E2F4, SREBF1, STAT6, CEBPB, KEAP1 and MYBBP1A) TFs encoding genes in the IPAH (Figure 2C). Then, we constructed the 22 hub-TFs centric PPI (yellow nodes in Figure 2B) from the original PPI. The 22 hub-TFs centric PPI included 220 nodes (Figure 2B, yellow nodes are TFs), indicating that these TFs substantially control this network.

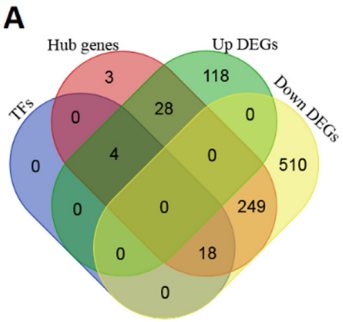

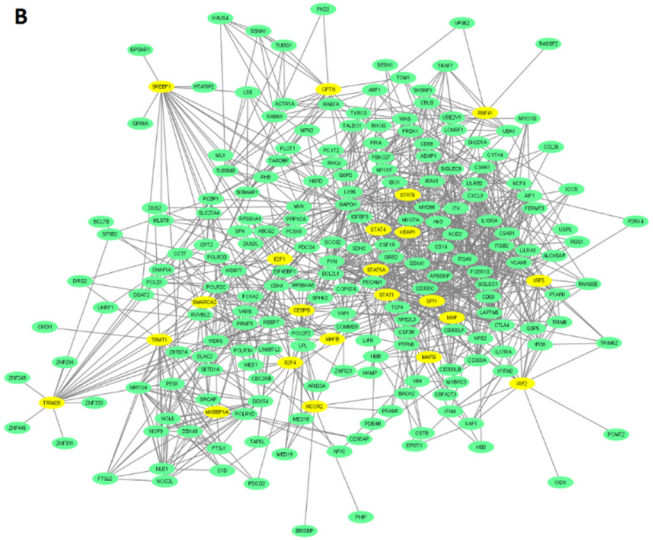

A. The 22 hub-TFs are deregulated in the IPAH

B. The hub-TFs centric PPI of DEGs identified by STRING and Cytoscape

C

Regulatory status	Entrez ID	Symbol	Combined ES	P value	Degree of interaction
Upregulated	6772	*STAT1*	0.78905	3.60E-02	46
	6775	*STAT4*	1.5946	1.16E-07	18
	10133	*OPTN*	0.95956	0.049303	15
	6595	*SMARCA2*	0.91287	0.0026744	14
Downregulated	6688	*SP1*	-1.3852	2.20E-06	57
	6720	*SREBF1*	-1.3275	6.26E-06	20
	9817	*KEAP1*	-1.283	1.23E-04	24
	3663	*IRF5*	-1.1861	5.91E-05	21
	4094	*MAF*	-1.1371	2.72E-02	20
	6778	*STAT6*	-0.78687	1.25E-02	22
	6776	*STAT5A*	-0.74051	2.15E-02	27
	10155	*TRIM28*	-0.72729	3.09E-02	20
	1051	*CEBPB*	-0.72171	2.60E-02	20
	55621	*TRMT1*	-1.1251	0.00013349	18
	1869	*E2F1*	-0.65677	0.049824	17
	3660	*IRF2*	-0.6628	0.047818	15
	10514	*MYBBP1A*	-0.7319	0.023448	15
	9612	*NCOR2*	-1.0163	0.03095	14
	10193	*RNF41*	-0.97401	0.0011227	12
	4097	*MAFG*	-0.70228	0.031446	11
	9935	*MAFB*	-0.84611	0.0065965	10
	1874	*E2F4*	-1.0899	0.00023419	10

C. The differential regulatory status of 22 hub-TFs with their degree of interactions

Figure 2. Identification and interaction of Hub-TFs.

3.3. Hub-TFs are associated with the enrichment of GOs and pathways

We inputted all deregulated hub-TFs into the GSEA software to identify the functional involvement of these TFs in the IPAH. The top ten biological processes (BPs) included positive regulation of the RNA metabolic process, positive regulation of the nucleobase-containing compound metabolic process, positive regulation of the cellular biosynthetic process, positive regulation of transcription by RNA polymerase II, negative regulation of transcription by RNA polymerase II, negative regulation of nucleobase containing compound metabolic process, negative regulation of the biosynthetic process, positive regulation of gene expression, response to oxygen-containing compound and defense response (Figure 3A). The other enriched BPs are illustrated in Supplementary Table S5. The enriched cellular components (CCs) are chromatin, Chromosome, transcription regulator complex, RNA polymerase II transcription regulator complex and nuclear protein-containing complex (Figure 3A). In addition, the top ten molecular functions (MFs) included Transcription regulator activity, CIS regulatory region sequence-specific DNA binding,

Sequence-specific DNA binding, DNA binding transcription activator activity, DNA binding transcription factor activity, Chromatin binding, Transcription factor binding, Identical protein binding, DNA binding transcription factor binding and RNA polymerase II specific DNA binding TF binding (Figure 3A). The other enriched MFs are illustrated in Supplementary Table S6.

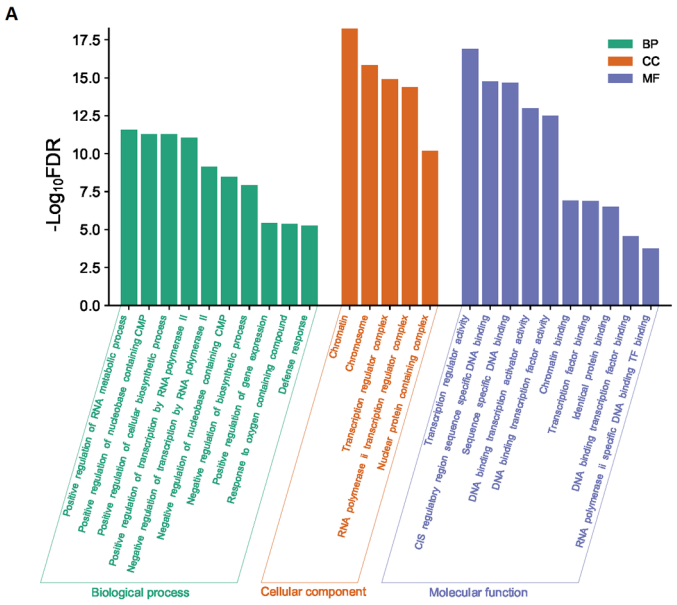

A. The top enriched biological processes, cellular components, and molecular functions are significantly associated with deregulated hub TFs in IPAH

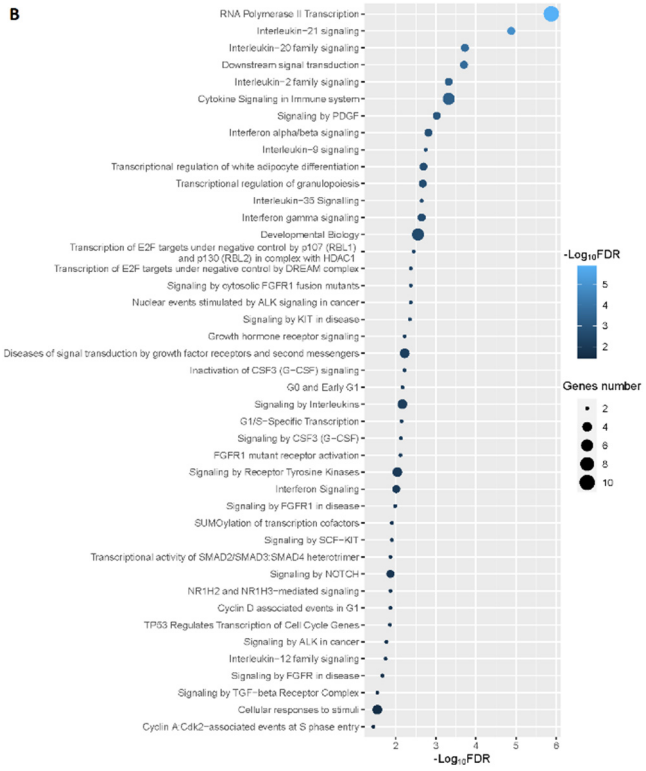

B. The enriched Reactome pathways are significantly associated with hub-TFs in IPAH

Figure 3. The involvement of deregulated TFs with the enrichment of functional activity in IPAH.

Moreover, we identified 43 significant Reactome pathways (Figure 3B) that are mainly involved in immune regulation (interleukin-21 signaling, interleukin-20 family signaling, cytokine signaling in immune system, interleukin-2 family signaling, signaling by PDGF, interferon alpha/beta signaling, interleukin-9 signaling, interferon gamma signaling, interleukin-35 signaling, signaling by interleukins, G1/S-Specific transcription, interferon signaling and interleukin-12 family signaling) and cellular signaling processes (RNA polymerase II transcription, downstream signal transduction, transcriptional regulation of white adipocyte differentiation, transcriptional regulation of granulopoiesis, developmental Biology, transcription of E2F targets under negative control by p107 (RBL1) and p130 (RBL2) in complex with HDAC1, signaling by cytosolic FGFR1 fusion mutants, Nuclear events stimulated by ALK signaling in cancer, transcription of E2F targets under negative control by DREAM complex, Signaling by KIT in disease, growth hormone receptor signaling, diseases of signal transduction by growth factor receptors and second messengers, inactivation of CSF3 (G-CSF) signaling, G0 and Early G1, signaling by CSF3 (G-CSF), FGFR1 mutant receptor activation, signaling by receptor tyrosine kinases, signaling by FGFR1 in disease, signaling by SCF-KIT, SUMOylation of transcription cofactors, transcriptional activity of SMAD2/SMAD3:SMAD4 heterotrimer, Cyclin D associated events in G1, NR1H2 and NR1H3-mediated signaling, Signaling by NOTCH, TP53 Regulates transcription of cell cycle genes, signaling by ALK in cancer, signaling by FGFR in disease, cellular responses to stimuli, signaling by TGF-beta receptor complex and cyclin A: Cdk2-associated events at S phase entry).

3.4. MiRNAs are differentially expressed in IPAH and associated with the co-regulatory network with Hub-TFs

We identified 17 upregulated (such as hsa-miR-505-5p, hsa-miR-183-5p, hsa-miR-375, hsa-miR-500a-3p, hsa-miR-6074, hsa-miR-152, hsa-miR-31-5p, hsa-miR-198 and hsa-miR-648) and 12 downregulated (such as hsa-miR-146b-3p, hsa-miR-1256, hsa-miR-302f, hsa-miR-517a-3p, hsa-miR-4693-5p, hsa-miR-4704-3p, hsa-miR-1178-3p, hsa-miR-495-5p, hsa-miR-1253 and hsa-miR-656) miRNAs in IPAH (Table 2). Then, we predicted the target genes of differentially expressed miRNAs. We revealed that the DEmiRs targeted the 8550 genes (Figure 4A). Interestingly, we found that the 16 hub-TFs encoding genes (E2F4, IRF2, MAF, RNF41, KEAP1, STAT1, TRIM28, MAFB, E2F1, CEBPB, NCOR2, MAFG, MYBBP1A, STAT6, OPTN and SMARCA2) involved in the interaction with DEmiRs (Figure 4B). For example, the TF TRIM28 interacted with five DEmiRs, included hsa-mir-199a-3p, hsa-mir-4473, hsa-mir-505-5p, hsa-mir-30a-5p, and hsa-mir-183-5p (Figure 4B). Similarly, the transcription factor MYBBP1A interacted with hsa-mir-26b-5p, hsa-mir-183-5p and hsa-mir-199a-3p (Figure 4B). It indicated that the co-regulatory network between the hub-TFs and miRNAs might play potential regulatory roles in the IPAH.

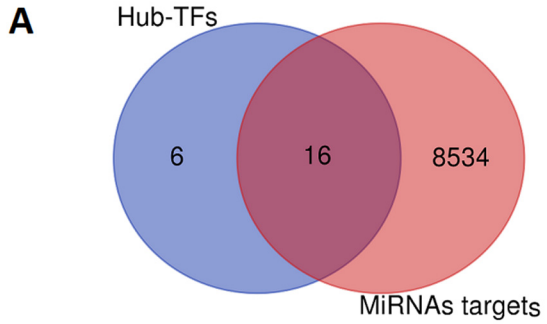

A. The Venn diagram identifies 16 hub-TFs associated with the interaction of DEmiRs

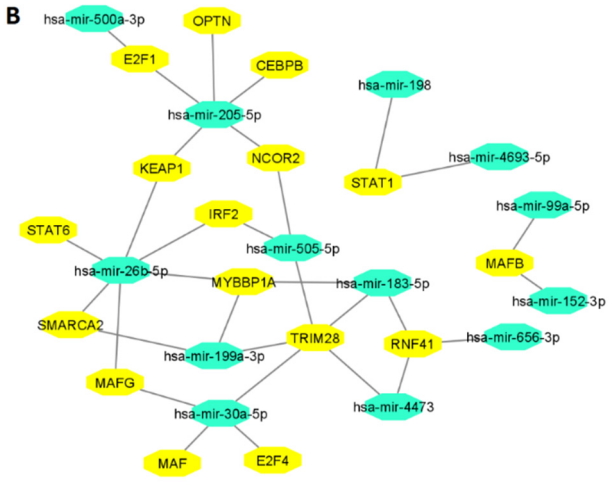

B. The co-regulatory network of the 16 hub-TFs with the DEmiRs. The yellow nodes indicated the hub-TFs, and another color indicated the DEmiRs in IPAH

Figure 4. Identification and construction of miRNAs-hub TFs co-regulatory network.

Table 2. DEmiRs in IPAH (LogFC > 1.0, and P Value < 0.05).

Regulatory status	MiRNAs	P Value	LogFC
	hsa-miR-505-5p	3.23×10^{-05}	7.178
	hsa-miR-183-5p	1.40×10^{-02}	4.585
	hsa-miR-375	3.63×10^{-02}	4.393
	hsa-miR-500a-3p	3.45×10^{-02}	4.057
	hsa-miR-6074	3.77×10^{-02}	3.888
Upregulated	hsa-miR-152-3p	3.83×10^{-02}	3.866
	hsa-miR-31-5p	3.69×10^{-02}	3.521
	hsa-miR-198	3.88×10^{-02}	3.397
	hsa-miR-648	4.12×10^{-02}	3.325
	hsa-miR-4473	4.04×10^{-02}	2.785
	hsa-miR-3974	3.71×10^{-02}	2.688

Continued on next page

Regulatory status	MiRNAs	P Value	LogFC
Downregulated	hsa-miR-205-5p	4.53×10^{-03}	2.525
	hsa-miR-99a-5p	2.34×10^{-02}	1.489
	hsa-miR-199a-3p	1.36×10^{-02}	1.481
	hsa-miR-199b-5p	4.16×10^{-02}	1.390
	hsa-miR-26b-5p	4.38×10^{-02}	1.282
	hsa-miR-30a-5p	4.83×10^{-02}	1.140
	hsa-miR-15b-3p	3.55×10^{-02}	−1.065
	hsa-miR-6716-3p	4.06×10^{-02}	−1.179
	hsa-miR-656	2.67×10^{-02}	−1.253
	hsa-miR-1253	3.79×10^{-02}	−2.638
	hsa-miR-495-5p	4.11×10^{-02}	−3.203
	hsa-miR-1178-3p	2.90×10^{-02}	−3.588
	hsa-miR-4704-3p	4.12×10^{-02}	−3.753
	hsa-miR-4693-5p	2.42×10^{-02}	−4.115
	hsa-miR-517a-3p	1.70×10^{-02}	−4.189
	hsa-miR-302f	1.03×10^{-02}	−4.408
	hsa-miR-1256	2.07×10^{-02}	−4.576
	hsa-miR-146b-3p	4.75×10^{-04}	−5.674

3.5. Validation of hub-TFs in the peripheral blood mononuclear cells of IPAH patients and their diagnostic efficacy in IPAH

The expression level of co-regulatory 16 hub-TFs was validated in the blood sample (GSE33463 [31]) of IPAH patients. We found that the expression levels of STAT1, MAF, CEBPB, MAFB, NCOR2 and MAFG are consistently differentially expressed in the peripheral blood mononuclear cells of IPAH patients compared with the control (Figure 5A). The expression level of STAT1 is elevated, and the expression level of MAF, CEBPB, MAFB, NCOR2 and MAFG is downregulated in the blood sample of IPAH patients. It indicates that these hub-TFs are crucial regulators in IPAH development and progression. Moreover, we evaluated the diagnostic efficacy (AUC > 0.05) of this validated hub-TFs encoding genes (STAT1, MAF, CEBPB, MAFB, NCOR2 and MAFG) in the peripheral blood mononuclear cells (GSE33463) of IPAH cohort (GSE33463). Interestingly, we found that the expression value clearly distinguished the IPAH cases from the control samples (AUC > 0.5) (Figure 5B). Furthermore, we verified the diagnostic efficacy of these hub-TFs encoding genes (STAT1, MAF, CEBPB, MAFB, NCOR2 and MAFG) in the lung tissues in IPAH cases (GSE117261). In lung tissues, the AUCs of all hub-TFs encoding genes ranged from 0.657 to 0.726, indicating their excellent diagnostic values for distinguishing IPAH cases and normal individuals. It suggested that these hub-TFs can be utilized to diagnose the IPAH cases from healthy individuals.

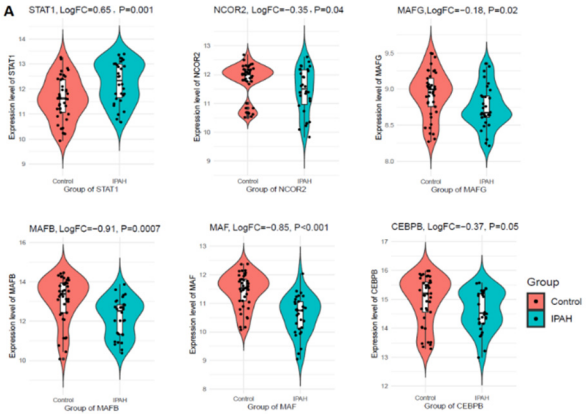

A. The six TFs encoding genes (STAT1, MAF, CEBPB, MAFB, NCOR2, and MAFG) are consistently differentially expressed in the peripheral blood mononuclear cells of IPAH patients. The expression level of STAT1is elevated, and the level of MAF, CEBPB, MAFB, NCOR2, and MAFG is downregulated in the blood sample of IPAH patients

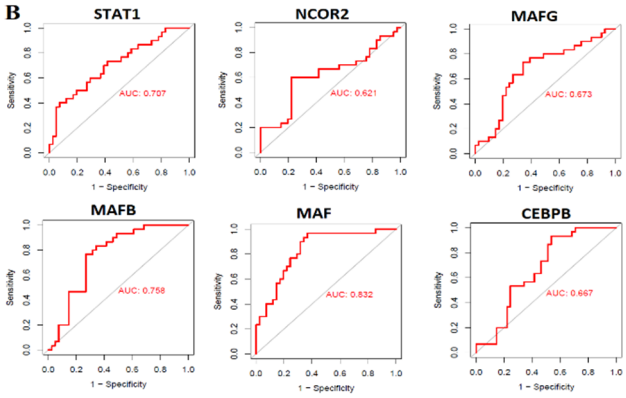

B. The expression value of six TFs encoding genes (STAT1, MAF, CEBPB, MAFB, NCOR2, and MAFG) in the peripheral blood mononuclear cells (GSE33463) showed the diagnostic efficacy between the IPAH and control samples

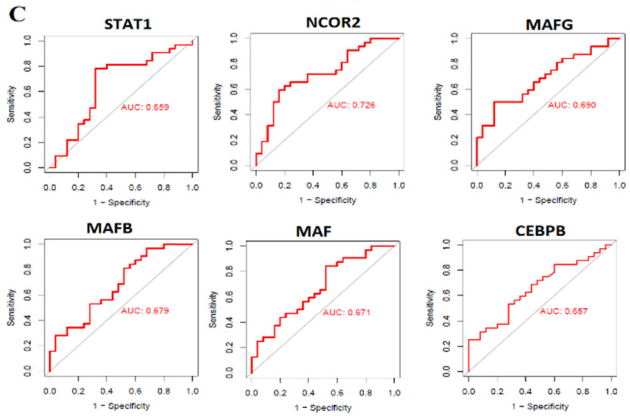

C. The expression value of six TFs encoding genes (STAT1, MAF, CEBPB, MAFB, NCOR2, and MAFG) in the lung tissues (GSE117261) showed the diagnostic efficacy between the IPAH and control samples

Figure 5. The validation of co-regulatory hub-TFs in the IPAH patients.

3.6. Immune infiltrations in the IPAH

Since potential biomarkers are associated with the immune infiltration IPAH [20], we identified the deregulated immune signatures between the IPAH and control. We found that the content of CD4 regulatory T cells, CAFs, CD8 regulatory T cells, endothelial cells, eosinophil, Th2 cells, pDC and Th17 cells are higher in IPAH than the control (Wilcoxon rank-sum test, $P < 0.05$) (Figure 6). In contrast, the content of pericytes, activated dendritic cells, epithelial cells, immature dendritic cells, macrophages and neutrophils are lower in IPAH (Wilcoxon rank-sum test, $P < 0.05$) (Figure 6).

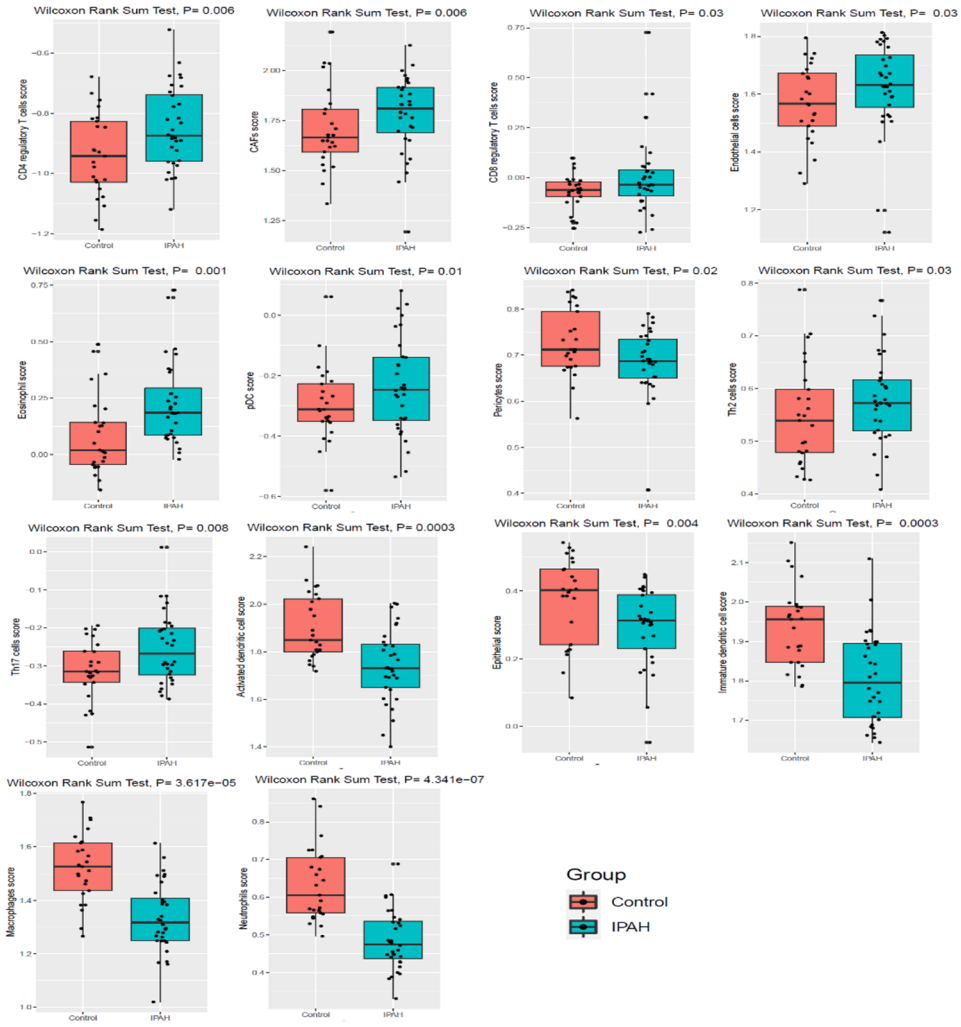

Figure 6. Immune signatures are significantly ($P < 0.05$) differentiated between the IPAH and healthy individuals.

3.7. Hub-TFs encoding genes are associated with immune infiltrations in the IPAH

Since hub-TFs are associated with the enrichment of the various immunological signatures (Figure 6), we anticipated that the hub-TFs encoding genes are correlated with immune infiltrations. To prove this hypothesis, we identified the ssGSEA score of various immune signatures that included B cells, CD4+ regulatory T cells, CD8+ regulatory T cells, eosinophil, immature B cells, immature

dendritic cells, macrophages, mast cells, monocytes, MDSCs, neutrophils, pDC, pericytes, Tfh, Th1, Th2, Tregs and smooth muscle. We revealed that the expression level of STAT1 is positively correlated (Spearman's correlation test, $R > 0.30$ and $P < 0.05$) with the infiltrations of CD4 regulatory T cells, immature B cells, macrophages, MDSCs, monocytes, Tfh cells and Th1 cells (Figure 7). In addition, CD4 regulatory T cells, immature B cells and B cells are negatively correlated with the expression levels of *MAFG* in IPAH (Figure 7). Similarly, plasmacytoid dendritic cells (pDC) infiltration is negatively correlated with the expression level of *MAF* in IPAH (Spearman's correlation test, $R > 0.30$ and $P < 0.05$) (Figure 7). Moreover, the expression level of *MAFB* is positively correlated with activated dendritic cells, M2 macrophages, and MDSCs and negatively associated with endothelial cells, eosinophil and NK cells (Spearman's correlation test, $R > 0.30$ and $P < 0.05$) (Figure 7). The expression level of NCOR2 is positively correlated with macrophages and negatively correlated with the infiltrations of B cells (Spearman's correlation test, $R > 0.30$ and $P < 0.05$) (Figure 7). CEBPB, other hub-TFs, is positively correlated with the infiltration of M2 macrophages and epithelial cells (Spearman's correlation test, $R > 0.30$ and $P < 0.05$) (Figure 7). Altogether, the validated hub-TFs are associated with the infiltrations of various immune signatures, including M2 Macrophages, MDSCs, CD4 regulatory T cells, immature B cells, endothelial cells, eosinophils, B cells and NK cells. It demonstrated that these hub-TFs are crucially associated with regulating immunity in IPAH patients.

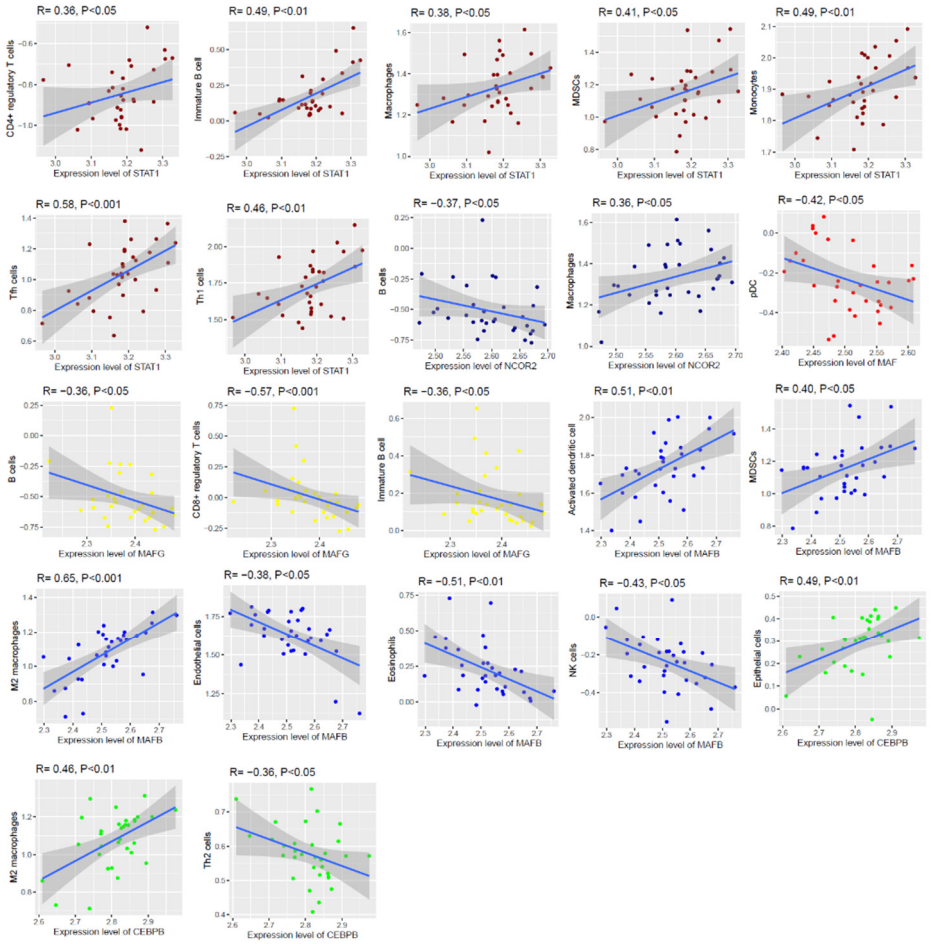

Figure 7. The co-regulatory hub-TFs are associated with immune infiltrations in the IPAH.

3.8. Interaction of drugs with hub-TFs and their molecular docking

We employed the DGIdb [45] to identify potential drugs associated with 6 validated hub-TFs (STAT1, MAF, CEBPB, MAFB, NCOR2 and MAFG). We identified that STAT1 interacts with 6 drugs, including garcinol, guttiferone k, picoplatin, cisplatin, CHEMBL85826 and ipriflavone (Figure 8A). Moreover, the NCOR2, another hub-TFs, potentially interacted with benzbromarone, CHEMBL312032 and 9, 10-phenanthrenequinone (Figure 8A). After getting this interaction, we anticipated that these drugs could potentially interact with the amino acid residues of the protein product of hub-TFs with a minimum binding affinity. To identify the interaction, we examined the molecular docking of these hub-TFs (STAT1 and NCOR2) with identified drugs. Interestingly, we found that the protein product of STAT1 is potentially interacting with the 5 drugs with a minimum binding affinity (binding affinity < −4.8) (Table 3). The protein product of STAT1 is bound with garcinol, guttiferone, picoplatin, CHEMBL85826, and ipriflavone with an appreciable binding affinity (Table 3). Guttiferone interacting with six amino acid residues (TYR A: 203, TYR A: 289, TYR A: 287, HIS A:291, GLU A:290, LYS A:200) of STAT1 (1YVL) with the minimum binding affinity-7.1 (Figure 8B and Table 3). The potential interaction of amino acid residues of STAT1 with garcinol, picoplatin, CHEMBL85826 and ipriflavone is displayed in Table 3. In addition, benzbromarone interacts with the five amino acid residues (LYS A: 10, LYS A: 44, TYR A: 42, LEU A: 48, MET A: 6) of the protein product of NCOR2 (Figure 8C and Table 3). Moreover, the potential interaction of amino acid residues of NCOR2 with CHEMBL312032 and 9, 10-phenanthrenequinone is displayed in Table 3.

Table 3. The binding affinity of interacting drugs with the amino acid residues of hub-TFs.

Protein products	Drugs	Binding Affinity	Interacting amino acid residues
STAT1 (1YVL)	Garcinol	−7.1	LEU A:109, ARG A:113, LEU A:116
	Guttiferone	−7.1	TYR A:203, TYR A:289, TYR A:287, HIS A:291, GLU A:290, LYS A:200
	Picoplatin	−4.8	TYR A:287, LYS A:286
	CHEMBL85826	−7.8	ASP A:207, TYR A:289, TYR A:203
	Ipriflavone	−7.0	GLN A:196, TYR A:289, TYR A:203, LEU A:199
NCOR2 (2LTP)	Benzbromarone	−6.9	LYS A:10, LYS A:44, TYR A:42, LEU A:48, MET A:6
	CHEMBL312032	−6.9	LYS A:44, TYR A:39, LEU A:48, LEU A:13, MET A:6, PHE A:48
	9,10-phenanthrenequinone	−7.2	LYS A:44, LEU A:48, MET A:6

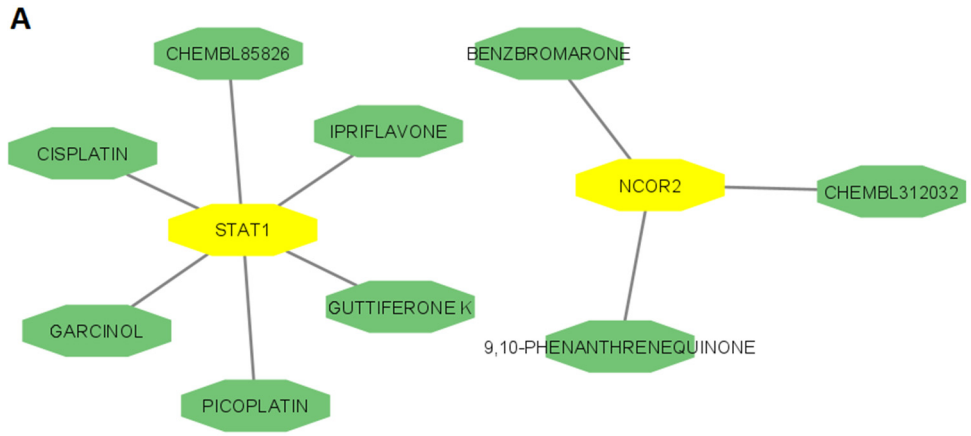

A. The Interaction of hub-TFs with drugs. The central yellow nodes are hub-TFs, and the green nodes indicate the drugs. We used the DGIdb database and the Cytoscape to identify drug interaction and visualization

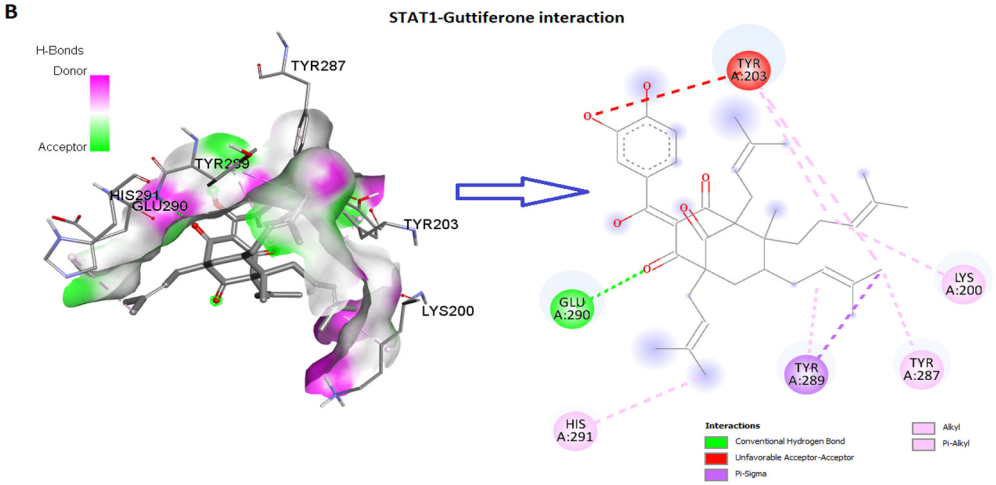

B. The 3D and 2D interaction of STAT1 and guttiferone in molecular docking study

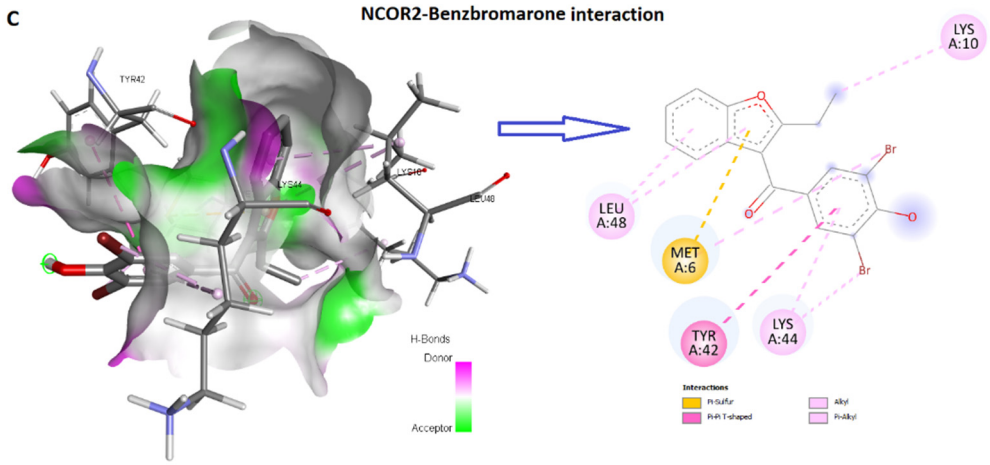

C. The 3D and 2D interaction of NCOR2 and benzbromarone in molecular docking study

Figure 8. The co-regulatory hub-TFs are associated with drug interaction.

4. Discussion

For the first time, we integrated three gene expression datasets (GSE48149 [26,27], GSE113439 [28], and GSE117261 [29,30]) to identify the deregulated TFs between the IPAH and control samples (Figure 1 and Table 1). Subsequently, we identified the hub-TFs encoding genes differentially expressed in IPAH (Figure 2A). Previous studies indicated that the identified hub-TFs are associated with the development and progression of pulmonary disease. For example, Yamamura et al. [47] discovered that the level of STAT1 is sustained longer times in pulmonary artery smooth muscle cells from patients with IPAH. The PDGF-induced activation of PDGF receptors is associated with STAT1-mediated signaling in pulmonary artery smooth muscle cell proliferation and vascular remodeling in patients with IPAH. Gairhe et al. [48] found that the activation of STAT1-mediated signaling correlates with the idiopathic PAH's pathogenesis. The activation of STAT4 is associated with the activation of the immune cells-mediated signaling process in chronic obstructive pulmonary disease [49]. The downregulated level of NCOR2 is involved with the enhanced expression of pro-tumorigenic genes in lung adenocarcinoma [50]. In IPAH patients, the reduced level of STAT5 is correlated with the pathogenesis of human disease [51]. The hub-TFs are substantially associated with functional enrichments (Figure 3). Similar to the previous studies, hub-TFs encoding genes are related to the enrichment of interleukin-21 signaling, cytokine signaling, and cell cycle-related signaling in PAH [52–54]. As expected, we found the enriched transcriptional signaling associated pathways, including RNA polymerase II transcription, downstream signal transduction, transcriptional regulation of white adipocyte differentiation, transcriptional regulation of granulopoiesis and transcriptional activity of SMAD2/SMAD3:SMAD4 heterotrimer. The interaction of human TF with genes can be stimulated the transcription-associated signaling pathways [55]. Altogether, these results suggested that the TFs encoding genes are critically associated with the pathogenesis and development of PAH.

Since miRNAs are substantially associated with the pathogenesis, development, and progression of pulmonary diseases [21,23], we identified the key miRNAs that are differentially expressed in IPAH. These key miRNAs are linked with the pathogenesis of lung and heart diseases. For example, the expression of hsa-miR-505 is significantly increased in hypertensive patients [56]. Hsa-miR-183-5p, the second top-upregulated miRNA, is increased in lung cancer, which influences the cell proliferation, migration, and cell cycle of NSCLC [57]. MiR-205 is a vital biomarker to detect and predict the recurrence of patients with lung cancer [58]. In lung cancer, the increased level of miR-205-5p promoted cellular proliferation and metastasis [59]. The expression level of MiR-1256 was downregulated in NSCLC, and the miR-1256/TCTN1 signaling axis can be played a crucial role in NSCLC [60].

Then, we discovered that potential TFs in hub-TFs-miRNA coregulatory networks are associated with the infiltrations of various immune signatures in IPAH (Figure 7). It was demonstrated that STAT1 is increased in a model of hypoxic pulmonary hypertension and idiopathic pulmonary fibrosis [61,62]. The STAT1/STAT3 signaling axis mediated the downstream mechanism of endothelial cell proliferation in IPAH [61]. In the rat model, the expression level of STAT1 is correlated with the infiltrations of immune cells in PAH [63]. Maf is the positive and negative regulator of cytokine gene expression by controlling the disease-specific downstream gene networks [64]. Therefore, the co-regulatory network of miRNAs with these hub-TFs may be associated with the downstream signaling to influence immunity in IPAH patients. In IPAH, the deregulated

biomarkers are related to the infiltrations of CD8+ T cells, macrophages, CD4+ T cells, monocytes and neutrophils [2]. Yang et al. [65] revealed the dysregulated immune reactions in the lung tissue of patients with IPAH. They found the various immune signatures positively and negatively correlated with the expression level of hub genes. Ni et al. [66] stated that the irregular immune cell distribution and polarization in the lung arterial vasculature are associated with the development and progression of PAH. The inflammatory and deregulated immune processes are crucially involved with the chemokines and cytokines-mediated complications in pulmonary arterial hypertension [67]. These previous studies strictly supported our findings. We revealed that immune signatures are significantly deregulated in IPAH (Figure 6), and hub-TFs encoding genes' expression level correlates with infiltrations of various immune signatures. Therefore, the hub-TFs-miRNA coregulatory networks (Figure 9), including hsa-miR-205-5p-CEBPB, hsa-miR-205-5p-NCOR2, hsa-miR-26b-5p-MAFG, hsa-miR-30a-5p-MAFG, hsa-miR-30a-5p-MAF, hsa-miR-152-3p- MAFB, hsa-miR-99a-5p-MAFB, hsa-miR-198-STAT1 and hsa-miR-4693-5p-STAT1 may be associated with the dysregulation of immune processes in IPAH. Additionally, the enrichment level of various immune-associated pathways (Figure 3) further supported the immunological association of these TFs in IPAH. Finally, we identified some potential drugs that interacted with the protein product of STAT1 and NCOR2. Potential drug repurposing is an important avenue to treat rare diseases, such as PAH and IPAH. This type of approach can combat the high costs of novel drug discovery and has an added safety benefit to existing drugs. Since IPAH is a rare disease, we revealed the interaction of the protein products of co-regulatory hub-TFs (STAT1 and NCOR2) with existing potential drugs. Masullo et al. [68] proposed that the direct interaction of garcinol and STAT1 can be modulated the cytokine signaling pathways in different cell lines. The same group of researchers revealed that the interaction of guttiferones K and STAT1 is associated with the inhibition of STAT1 for binding with DNA, which ultimately inhibits transcriptional signaling. Benzbromarone is interacting with NCOR2 and it was reported that the application of Benzbromarone leads to pulmonary vasodilation, which can be recognized by the decrease in pulmonary vascular resistance [52]. Toshner et al. reported that benzbromarone is utilized for the clinical trial of PAH [69]. In pulmonary arteries and pulmonary artery smooth muscle cells (PASMCs), benzbromarone significantly decreased the right ventricular pressure and reversed the remodeling of established pulmonary hypertension in animal models [70].

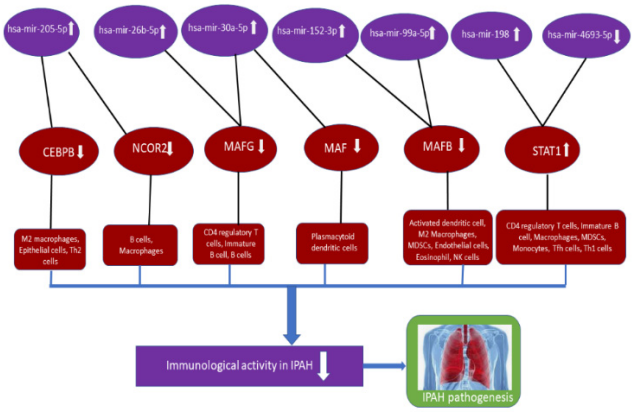

Figure 9. The deregulated miRNA-mRNA co-regulatory networks associated with immune infiltrations, immunological activities, and IPAH pathogenesis.

The drawback of our study is that the IPAH-associated miRNA-mRNA co-regulatory networks identified in the bioinformatics study have not been proven by clinical experimental validation. Thus, although our findings could provide potentially valuable biomarkers for IPAH development, diagnosis and therapeutic targets, future clinical and experimental validation would be needed to apply these results to the clinical application of IPAH treatment.

5. Conclusions

Identifying hub-TFs and miRNA- hub-TFs co-regulatory networks may provide new avenues into the IPAH development and pathogenesis mechanism. The coregulatory networks, including hsa-miR-205-5p-*CEBPB*, hsa-miR-205-5p-*NCOR2*, hsa-miR-26b-5p-*MAFG*, hsa-miR-30a-5p-*MAFG*, hsa-miR-30a-5p-*MAF*, hsa-miR-152-3p- *MAFB*, hsa-miR-99a-5p-*MAFB*, hsa-miR-198-*STAT1* and hsa-miR-4693-5p-*STAT1* are involving with the pathogenesis of IPAH.

Conflicts of Interest

The authors declare that they have no competing interests.

Funding statement

This study was funded by the Natural Science Foundation of China (grant number: 81860096).

References

1. M. M. Hoeper, M. Humbert, R. Souza, M. Idrees, S. M. Kawut, K. Sliwa-Hahnle, et al., A global view of pulmonary hypertension, *Lancet Respir. Med.*, **4** (2016), 306–322. https://doi.org/10.1016/s2213-2600(15)00543-3
2. H. Zeng, X. Liu, Y. Zhang, Identification of potential biomarkers and immune infiltration characteristics in idiopathic pulmonary arterial hypertension using bioinformatics analysis, *Front. Cardiovasc. Med.*, **8** (2021). https://doi.org/10.3389/fcvm.2021.624714
3. N. Galiè, M. Humbert, J. Vachiery, S. Gibbs, I. Lang, A. Torbicki, et al., 2015 ESC/ERS Guidelines for the Diagnosis and Treatment of Pulmonary Hypertension, *Rev. Esp. Cardiol. (Engl. Ed.)*, **69** (2016), 177. https://doi.org/10.1016/j.rec.2016.01.002
4. V. V. McLaughlin, M. D. McGoon, Pulmonary Arterial Hypertension, *Circulation*, **114** (2006), 1417–1431. https://doi.org/10.1161/CIRCULATIONAHA.104.503540
5. P. Pahal, S. Sharma, *Idiopathic Pulmonary Artery Hypertension*, StatPearls Publishing, Florida, 2022.
6. E. Spiekerkoetter, S. M. Kawut, V. A. de Jesus Perez, New and emerging therapies for pulmonary arterial hypertension, *Annu. Rev. Med.*, **70** (2019), 45–59. https://doi.org/10.1146/annurev-med-041717-085955
7. J. Y. Cao, K. M. Wales, R. Cordina, E. M. T. Lau, D. S. Celermajer, Pulmonary vasodilator therapies are of no benefit in pulmonary hypertension due to left heart disease: A meta-analysis, *Int. J. Cardiol.*, **273** (2018), 213–220. https://doi.org/10.1016/j.ijcard.2018.09.043

8. L. Yan, Q. Luo, Z. Zhao, Q. Zhao, Q. Jin, Y. Zhang, et al., Nocturnal hypoxia in patients with idiopathic pulmonary arterial hypertension, *Pulm. Circ.*, **10** (2020), 1–7. https://doi.org/10.1177/2045894019885364
9. N. W. Morrell, M. A. Aldred, W. K. Chung, C. G. Elliott, W. C. Nichols, F. Soubrier, et al., Genetics and genomics of pulmonary arterial hypertension, *Eur. Respir. J.*, **53** (2019), 1801899. https://doi.org/10.1183/13993003.01899-2018
10. M. A. Aldred, J. Vijayakrishnan, V. James, F. Soubrier, M. A. Gomez-Sanchez, G. Martensson, et al., BMPR2 gene rearrangements account for a significant proportion of mutations in familial and idiopathic pulmonary arterial hypertension, *Hum. Mutat.*, **27** (2006), 212–213. https://doi.org/10.1002/humu.9398
11. S. H. Choi, Y. Jung, J. Jang, S. Han, Idiopathic pulmonary arterial hypertension associated with a novel frameshift mutation in the bone morphogenetic protein receptor II gene and enhanced bone morphogenetic protein signaling, *Medicine*, **98** (2019), e17594. https://doi.org/10.1097/MD.0000000000017594
12. A. Chida, M. Shintani, T. Nakayama, Y. Furutani, E. Hayama, K. Inai, et al., Missense mutations of the BMPR1B (ALK6) gene in childhood idiopathic pulmonary arterial hypertension, *Circ. J.*, **76** (2012), 1501–1508. https://doi.org/10.1253/circj.cj-11-1281
13. D. Saygin, T. Tabib, H. E. T. Bittar, E. Valenzi, J. Sembrat, S. Y. Chan, et al., Transcriptional profiling of lung cell populations in idiopathic pulmonary arterial hypertension, *Pulm. Circ.*, **10** (2020), 1–15. https://doi.org/10.1177/2045894020908782
14. Y. Wu, J. Wharton, R. Walters, E. Vasilaki, J. Aman, L. Zhao, et al., The pathophysiological role of novel pulmonary arterial hypertension gene SOX17, *Eur. Respir. J.*, (2021). https://doi.org/10.1183/13993003.04172-2020
15. C. S. Park, S. H. Kim, H. Y. Yang, J. Kim, R. T. Schermuly, Y. S. Cho, et al., Sox17 deficiency promotes pulmonary arterial hypertension via HGF/c-Met signaling, *Circ. Res.*, **131** (2022), 792–806. https://doi.org/10.1161/CIRCRESAHA.122.320845
16. T. Wang, S. Wang, Y. Xu, C. Zhao, X. Qiao, C. Yang, et al., SOX17 loss-of-function mutation underlying familial pulmonary arterial hypertension, *Int. Heart. J.*, **62** (2021), 566–574. https://doi.org/10.1536/ihj.20-711
17. N. Zhu, C. L. Welch, J. Wang, P. M. Allen, C. Gonzaga-Jauregui, L. Ma, et al., Rare variants in SOX17 are associated with pulmonary arterial hypertension with congenital heart disease, *Genome Med.*, **56** (2018). https://doi.org/10.1186/s13073-018-0566-x
18. X. Yuan, Z. Wang, L. Wang, Q. Zhao, S. Gong, Y. Sun, et al., Increased levels of runt-related transcription factor 2 are associated with poor survival of patients with idiopathic pulmonary arterial hypertension, *Am. J. Men's Health.*, **14** (2020). https://doi.org/10.1177/1557988320945458
19. L. C. Price, S. J. Wort, F. Perros, P. Dorfmüller, A. Huertas, D. Montani, et al., Inflammation in pulmonary arterial hypertension, *Chest*, **141** (2012), 210–221. https://doi.org/10.1378/chest.11-0793
20. H. Zeng, X. Liu, Y. Zhang, Identification of potential biomarkers and immune infiltration characteristics in idiopathic pulmonary arterial hypertension using bioinformatics analysis, *Front. Cardiovasc. Med.*, **8** (2021). https://doi.org/10.3389/fcvm.2021.624714
21. I. Sarrion, L. Milian, G. Juan, M. Ramon, I. Furest, C. Carda, et al., Role of circulating miRNAs as biomarkers in idiopathic pulmonary arterial hypertension: Possible relevance of miR-23a, *Oxid. Med. Cell. Longevity*, **2015** (2015), 792846. https://doi.org/10.1155/2015/792846

22. W. He, X. Su, L. Chen, C. Liu, W. Lu, T. Wang, et al., Potential biomarkers and therapeutic targets of idiopathic pulmonary arterial hypertension, *Physiol. Rep.*, **10** (2022), e15101. https://doi.org/10.14814/phy2.15101
23. C. Li, Z. Zhang, Q. Xu, R. Shi, Comprehensive analyses of miRNA-mRNA network and potential drugs in idiopathic pulmonary arterial hypertension, *BioMed Res. Int.*, **2020** (2020), 5156304. https://doi.org/10.1155/2020/5156304
24. S. Hao, P. Jiang, L. Xie, G. Xiang, Z. Liu, W. Hu, et al., Essential genes and MiRNA-mRNA network contributing to the pathogenesis of idiopathic pulmonary arterial hypertension, *Front. Cardiovasc. Med.*, **8** (2021), 627873. https://doi.org/10.3389/fcvm.2021.627873
25. D. Li, A. Tulahong, M. N. Uddin, H. Zhao, H. Zhang, Meta-analysis identifying epithelial-derived transcriptomes predicts poor clinical outcome and immune infiltrations in ovarian cancer, *Math. Biosci. Eng.*, **18** (2021), 6527–6551. https://doi.org/10.3934/mbe.2021324
26. E. Hsu, H. Shi, R. M. Jordan, J. Lyons-Weiler, J. M. Pilewski, C. A. Feghali-Bostwick, Lung tissues in patients with systemic sclerosis have gene expression patterns unique to pulmonary fibrosis and pulmonary hypertension, *Arthritis Rheum.*, **63** (2011), 783–794. https://doi.org/10.1002/art.30159
27. L. Renaud, W. A. da Silveira, N. Takamura, G. Hardiman, C. Feghali-Bostwick, Prominence of IL6, IGF, TLR, and bioenergetics pathway perturbation in lung tissues of scleroderma patients with pulmonary fibrosis, *front. immunol.*, **11** (2020), 383. https://doi.org/10.3389/fimmu.2020.00383
28. M. Mura, M. J. Cecchini, M. Joseph, J. T. Granton, Osteopontin lung gene expression is a marker of disease severity in pulmonary arterial hypertension, *Respirology*, 24 (2019), 1104–1110. https://doi.org/10.1111/resp.13557
29. R. S. Stearman, Q. M. Bui, G. Speyer, A. Handen, A. R. Cornelius, B. B. Graham, et al., Systems analysis of the human pulmonary arterial hypertension lung transcriptome, *Am. J. Respir. Cell Mol. Biol.*, **60** (2019), 637–649. https://doi.org/10.1165/rcmb.2018-0368OC
30. C. E. Romanoski, X. Qi, S. Sangam, R. R. Vanderpool, R.S. Stearman, A. Conklin, et al., Transcriptomic profiles in pulmonary arterial hypertension associate with disease severity and identify novel candidate genes, *Pulm. Circ.*, **10** (2020). https://doi.org/10.1177/2045894020968531
31. C. Cheadle, A. E. Berger, S. C. Mathai, D. N. Grigoryev, T. N. Watkins, Y. Sugawara, et al., Erythroid-specific transcriptional changes in PBMCs from pulmonary hypertension patients, PloS One., **7** (2012), e34951. https://doi.org/10.1371/journal.pone.0034951
32. D. Wu, C. C. Talbot, Q. Liu, Z. Jing, R. L. Damico, R. Tuder et al., Identifying microRNAs targeting Wnt/β-catenin pathway in end-stage idiopathic pulmonary arterial hypertension, *J. Mol. Med.*, **94** (2016), 875–885. https://doi.org/10.1007/s00109-016-1426-z
33. J. Xia, E. E. Gill, R. E. W. Hancock, NetworkAnalyst for statistical, visual and network-based meta-analysis of gene expression data, *Nat. Protoc.*, **10** (2015), 823–844. https://doi.org/10.1038/nprot.2015.052
34. W. E. Johnson, C. Li, A. Rabinovic, Adjusting batch effects in microarray expression data using empirical bayes methods, *Biostatistics*, **8** (2007), 118–127. https://doi.org/10.1093/biostatistics/kxj037

35. M. E. Ritchie, B. Phipson, D. Wu, Y. Hu, C. W. Law, W. Shi, et al., limma powers differential expression analyses for RNA-sequencing and microarray studies, *Nucleic Acids Res.*, **43** (2015), e47. https://doi.org/10.1093/nar/gkv007
36. A. Subramanian, P. Tamayo, V. K. Mootha, S. Mukherjee, B. L. Ebert, M. A. Gillette, et al., Gene set enrichment analysis: a knowledge-based approach for interpreting genome-wide expression profiles, *PNAS*, **102** (2005), 15545–15550. https://doi.org/10.1073/pnas.0506580102
37. D. Szklarczyk, A. L. Gable, D. Lyon, A. Junge, S. Wyder, J. Huerta-Cepas, et al., STRING v11: protein-protein association networks with increased coverage, supporting functional discovery in genome-wide experimental datasets, *Nucleic Acids Res.*, **47** (2019), 607–613. https://doi.org/10.1093/nar/gky1131
38. C. Chin, S. Chen, H. Wu, C. Ho, M. Ko, C. Lin, CytoHubba: identifying hub objects and sub-networks from complex interactome, *BMC Syst. Biol.*, **8** (2014), S11. https://doi.org/10.1186/1752-0509-8-S4-S11
39. J. Wang, R. Akter, M. F. Shahriar, M. N. Uddin, Cancer-Associated Stromal Fibroblast-Derived Transcriptomes Predict Poor Clinical Outcomes and Immunosuppression in Colon Cancer, *Pathol. Oncol. Res.*, (2022). https://doi.org/10.3389/pore.2022.1610350
40. P. Shannon, A. Markiel, O. Ozier, N. S. Baliga, J. T. Wang, D. Ramage, et al., Cytoscape: a software environment for integrated models of biomolecular interaction networks, *Genome Res.*, **13** (2003), 2498–2504. https://doi.org/10.1101/gr.1239303
41. Y. Fan, K. Siklenka, S. K. Arora, P. Ribeiro, S. Kimmins, J. Xia, MiRNet-dissecting miRNA-target interactions and functional associations through network-based visual analysis, *Nucleic Acids Res.*, **44** (2016), 135–141. https://doi.org/10.1093/nar/gkw288
42. X. Robin, N. Turck, A. Hainard, N. Tiberti, F. Lisacek, J. Sanchez, M. Müller, PROC: an open-source package for R and S+ to analyze and compare ROC curves, *BMC Bioinformatics*., **77** (2011). https://doi.org/10.1186/1471-2105-12-77
43. J. Wang, M. N. Uddin, J. Hao, R. Chen, Y. Xiang, D. Xiong, et al., Identification of potential novel prognosis-related genes through transcriptome sequencing, bioinformatics analysis, and clinical validation in acute myeloid leukemia, *Front. Genet.*, **12** (2021). https://doi.org/10.3389/fgene.2021.723001
44. M. N. Uddin, R. Akter, M. Li, Z. Abdelrahman, Expression of SARS-COV-2 cell receptor gene ACE2 is associated with immunosuppression and metabolic reprogramming in lung adenocarcinoma based on bioinformatics analyses of gene expression profiles, *Chem. Biol. Interact.*, **335** (2021), 109370. https://doi.org/10.1016/j.cbi.2021.109370
45. K. C. Cotto, A. H. Wagner, Y. Feng, S. Kiwala, A. C. Coffman, G. Spies, et al., DGIdb 3.0: A redesign and expansion of the drug-gene interaction database, *Nucleic Acids Res.*, **46** (2018), 1068–1073. https://doi.org/10.1093/nar/gkx1143
46. X. Mao, Z. Ren, G. N. Parker, H. Sondermann, M. A. Pastorello, W. Wang, et al., Structural bases of unphosphorylated STAT1 association and receptor binding, *Mol. Cell*, **17** (2005), 761–771. https://doi.org/10.1016/j.molcel.2005.02.021
47. A. Yamamura, M. J. Nayeem, A. A. Mamun, R. Takahashi, H. Hayashi, M. Sato, Platelet-derived growth factor up-regulates Ca2+-sensing receptors in idiopathic pulmonary arterial hypertension, *FASEB J.*, **33** (2019), 7363–7374. https://doi.org/10.1096/fj.201802620R

48. S. Gairhe, K. S. Awad, E. J. Dougherty, G. A. Ferreyra, S. Wang, Z. Yu, et al., Type I interferon activation and endothelial dysfunction in caveolin-1 insufficiency-associated pulmonary arterial hypertension, *PNAS*, **118** (2021). https://doi.org/10.1073/pnas.2010206118
49. A. D. Stefano, G. Caramori, A. Capelli, I. Gnemmi, F. L. Ricciardolo, T. Oates, et al., STAT4 activation in smokers and patients with chronic obstructive pulmonary disease, *Eur. Respir. J.*, **24** (2004), 78–85. https://doi.org/10.1183/09031936.04.00080303
50. H. Alam, N. Li, S. S. Dhar, S. J. Wu, J. Lv, K. Chen, et al., HP1γ promotes lung adenocarcinoma by downregulating the transcription-repressive regulators NCOR2 and ZBTB7A, *Cancer Res.*, **78** (2018), 3834–3848. https://doi.org/10.1158/0008-5472.CAN-17-3571
51. Y. Yang, H. Yuan, J. G. Edwards, Y. Skayian, K. Ochani, E. J. Miller, et al., Deletion of STAT5a/b in vascular smooth muscle abrogates the male bias in hypoxic pulmonary hypertension in mice: Implications in the human disease, *Mol. Med.*, **20** (2014), 625–638. https://doi.org/10.2119/molmed.2014.00180
52. T. Hashimoto-Kataoka, N. Hosen, T. Sonobe, Y. Arita, T. Yasui, T. Masaki, et al., Interleukin-6/interleukin-21 signaling axis is critical in the pathogenesis of pulmonary arterial hypertension, *PNAS*, **112** (2015), 2677–2686. https://doi.org/10.1073/pnas.1424774112
53. E. Zhao, H. Xie, Y. Zhang, Identification of differentially expressed genes associated with idiopathic pulmonary arterial hypertension by integrated bioinformatics approaches, *J. Comput. Biol.*, **28** (2021), 79–88. https://doi.org/10.1089/cmb.2019.0433
54. W. Wang, Z. Jiang, D. Zhang, L. Fu, R. Wan, K. Hong, Comparative transcriptional analysis of pulmonary arterial hypertension associated with three different diseases, *Front. Cell Dev. Biol.*, **9** (2021). https://doi.org/10.3389/fcell.2021.672159
55. H. Göös, M. Kinnunen, K. Salokas, Z. Tan, X. Liu, L. Yadav, et al., Human transcription factor protein interaction networks, *Nat. Commun.*, **13** (2022), 766. https://doi.org/10.1038/s41467-022-28341-5
56. Q. Yang, C. Jia, P. Wang, M. Xiong, J. Cui, L. Li, et al., MicroRNA-505 identified from patients with essential hypertension impairs endothelial cell migration and tube formation, *Int. J. Cardiol.*, **177** (2014), 925–934. https://doi.org/10.1016/j.ijcard.2014.09.204
57. H. Wang, Z. Ma, X. Liu, C. Zhang, Y. Hu, L. Ding, et al., MiR-183-5p is required for non-small cell lung cancer progression by repressing PTEN, *Biomed. Pharmacother.*, **111** (2019), 1103–1111. https://doi.org/10.1016/j.biopha.2018.12.115
58. J. Li, S. Sun, N. Li, P. Lv, S. Xie, P. Wang, MiR-205 as a promising biomarker in the diagnosis and prognosis of lung cancer, *Oncotarget*, **8** (2017), 91938–91949. https://doi.org/10.18632/oncotarget.20262
59. Y. Zhao, J. Zhang, J. Yang, Y. Wei, J. Peng, C. Fu, et al., MiR-205-5p promotes lung cancer progression and is valuable for the diagnosis of lung cancer, *Thorac Cancer*, **13** (2022), 832–843. https://doi.org/10.1111/1759-7714.14331
60. W. Liu, X. Wan, Z. Mu, F. Li, L. Wang, J. Zhao, et al., MiR-1256 suppresses proliferation and migration of non-small cell lung cancer via regulating TCTN1, *Oncol. Lett.*, **16** (2018), 1708–1714. https://doi.org/10.3892/ol.2018.8794
61. H. El Chami, P. M. Hassoun, Immune and inflammatory mechanisms in pulmonary arterial hypertension, *Prog. Cardiovasc. Dis.*, **55** (2012), 218–228. https://doi.org/10.1016/j.pcad.2012.07.006

62. N. M. Patel, S. M. Kawut, S. Jelic, S. M. Arcasoy, D. J. Lederer, A. C. Borczuk, Pulmonary arteriole gene expression signature in idiopathic pulmonary fibrosis, *Eur. Respir. J.*, **41** (2013), 1324–1330. https://doi.org/10.1183/09031936.00084112
63. H. Yang, Y. Lu, H. Yang, Y. Zhu, Y. Tang, L. Li, et al., Integrated weighted gene co-expression network analysis uncovers STAT1(signal transducer and activator of transcription 1) and IFI44L (interferon-induced protein 44-like) as key genes in pulmonary arterial hypertension, *Bioengineered*, **12** (2021), 6021–6034. https://doi.org/10.1080/21655979.2021.1972200
64. L. Gabryšová, M. Alvarez-Martinez, R. Luisier, L. S. Cox, J. Sodenkamp, C. Hosking, et al., C-Maf controls immune responses by regulating disease-specific gene networks and repressing IL-2 in CD4+ T cells, *Nat. Immunol.*, **19** (2018), 497–507. https://doi.org/10.1038/s41590-018-0083-5
65. X. Yang, C. Wang, Y. Lin, P. Zhang, Identification of crucial hub genes and differential T cell infiltration in idiopathic pulmonary arterial hypertension using bioinformatics strategies, *Front. Mol. Biosci.*, **9** (2022). https://doi.org/10.3389/fmolb.2022.800888
66. S. Ni, T. Ji, J. Dong, F. Chen, H. Feng, H. Zhao, et al., Immune cells in pulmonary arterial hypertension, *Heart Lung Circ.*, **31** (2022), 934–943. https://doi.org/10.1016/j.hlc.2022.02.007
67. M. Rabinovitch, C. Guignabert, M. Humbert, M. R. Nicolls, Inflammation and immunity in the pathogenesis of pulmonary arterial hypertension, *Circ. Res.*, **115** (2014), 165–175. https://doi.org/10.1161/CIRCRESAHA.113.301141
68. M. Masullo, M. Menegazzi, S. Di Micco, P. Beffy, G. Bifulco, M. Dal Bosco, et al., Direct interaction of garcinol and related polyisoprenylated benzophenones of Garcinia cambogia fruits with the transcription factor STAT-1 as a likely mechanism of their inhibitory effect on cytokine signaling pathways, *J. Nat. Prod.*, **77** (2014), 543–549. https://doi.org/10.1021/np400804y
69. M. Toshner, E. Spiekerkoetter, H. Bogaard, G. Hansmann, S. Nikkho, K. W. Prins, Repurposing of medications for pulmonary arterial hypertension, *Pulm. Circ.*, **10** (2020). https://doi.org/10.1177/2045894020941494
70. R. Papp, C. Nagaraj, D. Zabini, B. M. Nagy, M. Lengyel, D. S. Maurer, et al., Targeting TMEM16A to reverse vasoconstriction and remodelling in idiopathic pulmonary arterial hypertension, *Eur. Respir. J.*, **53** (2019). https://doi.org/10.1183/13993003.00965-2018

AIMS Press